GEOPHYSICAL RESEARCH LETTERS, VOL. 18, NO. 9, PAGES 1767-1770, SEPTEMBER 1991

SHALLOW FAULTS MAPPED WITH SEISMIC REFLECTIONS: LOST RIVER FAULT, IDAHO

x

Mubarik Ali

Department of Earth Sciences, Quaid-i-Azam University

Richard D. Miller, and Don W. Steeples

Kansas Geological Survey, The University of Kansas

Abstract. A high-resolution seismic-reflection survey, conducted at the intersection of Arentson Gulch road and the western splay of the Lost River fault scarp in central Idaho, defines a bedrock surface about 80 m deep which is segmented by several faults forming graben structures. Six meters of total fault displacement can be interpreted on the bedrock reflector while only 1 to 2 m of displacement can be observed on a shallower refracting interface and the surface fault scarp. This relatively small displacement suggests the western splay has either been active only recently or extremely infrequently since deposition of the bedrock, or that strike-slip motion may be present. A westward deflection of the major activity along the Lost River fault was probably responsible for the gap in 1983 surface faulting between the Warm Spring and Thousand Springs segments. The inconsistency in total bed displacement based on reflection, refraction, and fault-scarp evidence suggests tectonic activity on the western splay spans more than just a single episode.

Introduction

Shallow faults considered to be probable future hazards in the Intermountain Seismic Belt are commonly buried beneath unconsolidated sediments. The location and offset of these subsurface shallow faults in many cases can be determined with seismic-reflection surveys.

The seismic survey discussed here was conducted at the intersection of Arentson Gulch road and the Lost River fault scarp (Figure 1). The purpose of the study was to delineate shallow subsurface structure. Arentson Gulch road is subparallel to Doublespring Pass road and about 9 miles to the northwest.

The 36 km of ground breakage in 1983 along the Lost River fault between Thousand Spring valley and the Lost River range in Idaho has been described as a reactivation of a set of shallow normal faults [Crone and Machette, 1984; Hait and Scott, 1978; Hait, 1985; Crone et al., 1987]. Earth-penetrating radar data collected across the scarp at the Doublespring Pass road suggest that more than just the 1983 faulting event was responsible for fractures and fill material less than 4 m deep [Bilham, 1985]. The upper 70 m of the fault zone at Doublespring Pass road was examined with high resolution seismic reflection within a month of the 1983 event [Miller and Steeples, 1986]. The fault zone in the upper 50 m at Doublespring Pass road is 180 m wide and predominantly composed of normal faults of varied ages [Treadway et al., 1988].

Geology

Borah Peak and Dickey Peak are located in the Lost River Range and demonstrate classical basin-range topography in Idaho. The topographic relief of the Lost River Range has
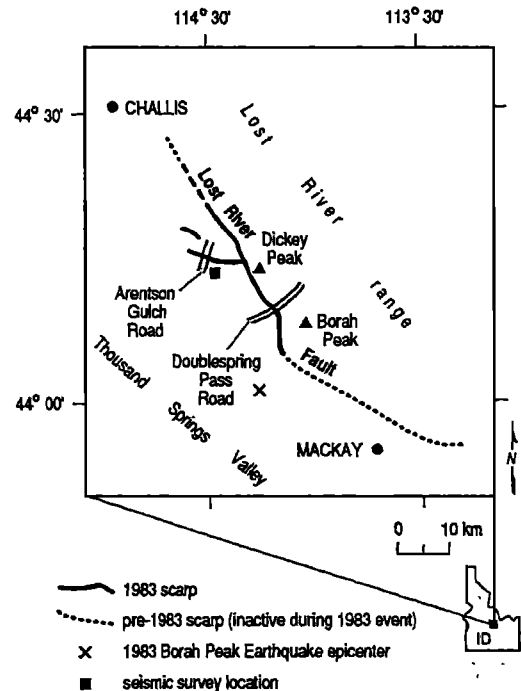
Fig. 1. Study area [modified from Crone et al., 1989].

been described as primarily due to an extended period of normal faulting beginning during middle Miocene and continuing through Holocene [Scott et al., 1985]. Much of the present topographic relief is probably the result of activity during late Pliocene and Pleistocene [Baldwin, 1951]. The Lost River Range is composed of complexly folded and faulted strata ranging in age from Proterozoic to early Pennsylvanian. The Lost River fault, identified as a range front fault, is typical of the Basin and Range structural province north of the Snake River Plain [Baldwin, 1951].

The 1983 earthquake produced 36 km of northwest-trending surface rupture predominantly along the Lost River fault. Of the 36 km, 14.2 km are found along a west-trending splay diverging from the range front fault at the base of Dickey Peak, extending through the alluvial valley at Arentson Gulch, across a series of bedrock hills, and out into Antelope Flat. The scars at Arentson Gulch and at the crest of the bedrock hills suggest a deeper zone of tectonic movement [Crone et al., 1985]. The average throw along the west-trending fault splay is less than half a meter. At Arentson Gulch road, however, the scarp possesses as much as 1.6 m of throw.

Data Acquisition and Processing

A single 225-m long seismic line with 2-m station spacing was acquired perpendicular to the fault scarp (Table 1). The data were collected along an access road that loosely follows topographic gradient, (i.e., northeast-southwest). The break

Copyright 1991 by the American Geophysical Union.

in slope at location 160 marks the fault scarp location (Figure 3).

Table 1. Field Parameters

Source	.50-caliber rifle
Source-receiver geometry	End-on
Source-to-nearest-receiver offset	24 meters
Source-to-farthest-receiver offset	70 meters
Source interval	2 meters
Receiver interval	2 meters
Maximum fold	12
Geophones per channel	3-40 Hz (in series)

Data were recorded on a 24-channel, fixed gain, 12-bit digital seismograph (Input/Output DHR-2400). Before digital sampling, the data were high-cut filtered (-3 dB at 1000 Hz with 24 dB/octave rolloff) anti-alias filtered (-60 dB at 2000 Hz with 60 dB/octave roll-off), and low-cut filtered, (-3 dB at 110 Hz with 24 dB/octave roll-off). The 250-ms records were digitized at a sampling interval of 0.5 ms.

The resolving power of seismic-reflection data depends on the surface station spacing, the recorded reflection frequency spectrum, and the size of the Fresnel zone at the reflector depth. Resolution limit of fault displacement is determined by dominant frequency of the seismic reflection and by seismic velocity. The detection limit and the uncertainty for fault displacement are about 1/10 of a wavelength, which is one meter or less for the data shown here.

Data processing was done on a 32-bit Data General computer at the Kansas Geological Survey. The processing flow was similar to those used on seismic data for petroleum exploration. Differences include more care in pre-reflection and air-wave energy muting, detailed NMO velocity analysis, and constraints imposed on statics corrections. Deconvolution of the data was not necessary due to a lack of prominent multiple-reflection energy and a low signal-to-noise ratio.

The elevation statics were applied with respect to a sloping datum generally parallel to the ground surface. The sloping datum was used to reduce the magnitude of the corrections, therefore reducing inherent error [Treadway et al., 1988]. Subtle horizontal shifts in shallow subsurface points as a function of depth (remnants of sloping datum corrections) are negligible on this survey.

Interpretation

Two complementary interpretations are presented here, one based on reflection information and the other on refraction information from the same seismic data set. The reflection-derived information is from depths of 50 to 90 m.

Reflection. Reflected energy at frequencies in excess of 100 Hz can be observed at 140 ms on unprocessed field files (Figure 2). The amplitude of ground-roll energy on some files is sufficiently high that it is difficult to confidently identify reflection energy. The general character of reflected energy across the line varies due to relative changes in noise levels, differences in physical characteristics of surficial material, and variations in source-and-receiver ground coupling.

A relatively coherent reflection event can be interpreted on the stacked data between 130 and 140 ms (Figure 3). This reflection is probably from the Paleozoic carbonate bedrock. Breaks in coherency can be observed in the reflection event between stations 170 and 195, 133 and 155, and 96 and 105. Reflection wavelet characteristics vary considerably between stations 185 to 195 and between 132 and 155.

Wavelet variability observed in the reflection event can be caused by changes in velocity (corresponding to lateral change in lithology), wide-angle reflections, uncompensated static correction, and/or extreme changes in the orientation of the
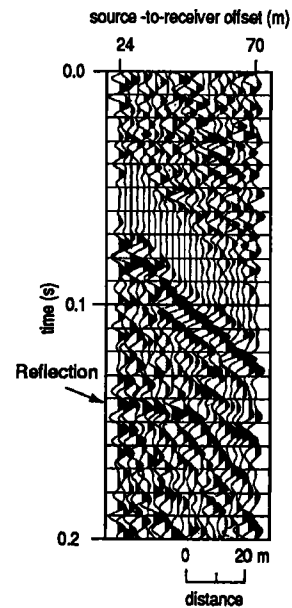

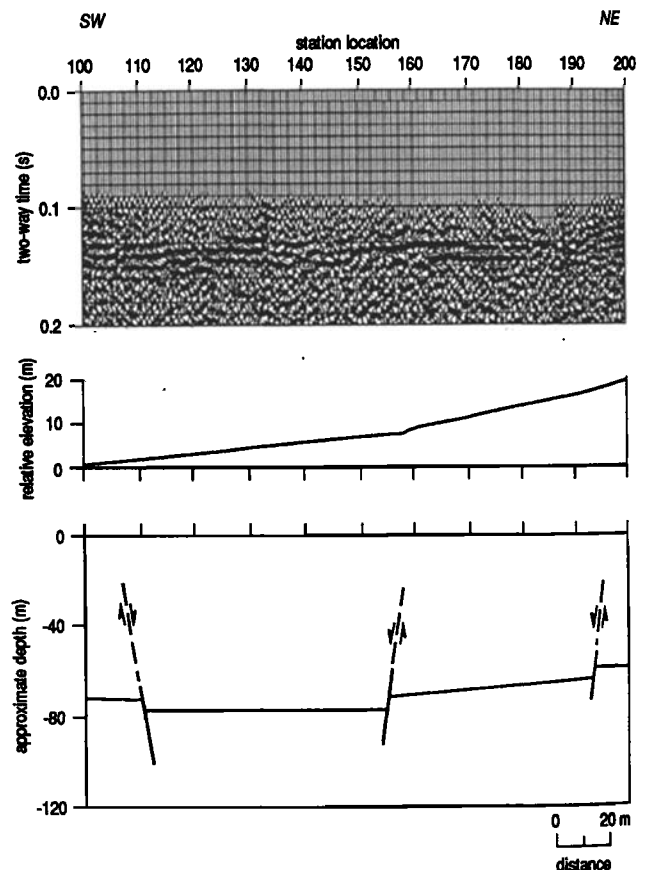Fig. 2. The filtered field file shows a reflection at 140 ms.

Fig. 3. A reflection at 130 ms can be observed across most of the 12-fold CDP stacked section.

reflector [Pullan and Hunter, 1985]. The relative influence of these factors cannot be established with existing data in this tectonically active area. It is likely, however, that all of them contribute to the wavelet variability. Effects of the variable near-surface have been reduced through careful muting, editing, and velocity/static corrections.

Stacking velocities are relatively consistent (approximately 1200 m/s) from station 115 to 201. The velocity decreases at station 115 to 1050 m/s, increasing gradually to 1100 m/s on the southwestern end of the line. The drop in velocity is probably related to either a change in lithology or tectonically altered physical properties of the material.

Refraction. Near-surface variations that show up as changes in refracted energy can sometimes be suggestive of shallow structural features. Unique depth determinations derived from refraction energy are not possible on CDP data collected using an end-on source/receiver configuration because the profile is not shot in both directions. Refracted seismic energy arrivals from unreversed profiles on this survey were used, however, to roughly locate distinct and/or rapid changes in subsurface properties within the upper 10 m (Figure 4).

The CDP data were sorted into a common-offset refraction section to portray variations in the shallow refracting interface (Figure 5). The geophone 46 m from the source received refractions (800 m/s) as first arrivals, therefore possessing the potential of detecting discontinuities in a near-surface layer shallower than 10 m.

The common offset refraction section suggests apparent arrival-time variations between stations 113 and 195. Assuming horizontally constant V_0 and V_1, the depth of the near-surface interface can be determined using a simple equation:

$$Z_i = ti \frac{V_0 V_1}{2\sqrt{V_1^2 - V_0^2}}$$

where $ti = Ti - X/V1$ and Ti is the intercept time for the refracted waves.

For the common offset section displayed, X=46 m (constant), V_0=500 m/s, and V_1=800 m/s are also assumed constant. Thus, X/V_1 and

$$V_0 V_1 / 2\sqrt{V_1^2 - V_0^2}$$

being invariants simplify the depth determination for this section.

Visible disruption in the refracted signal between locations 160 and 163 are probably related to the surface fault scarp produced by the Idaho earthquake of 1983 (Figure 5). The
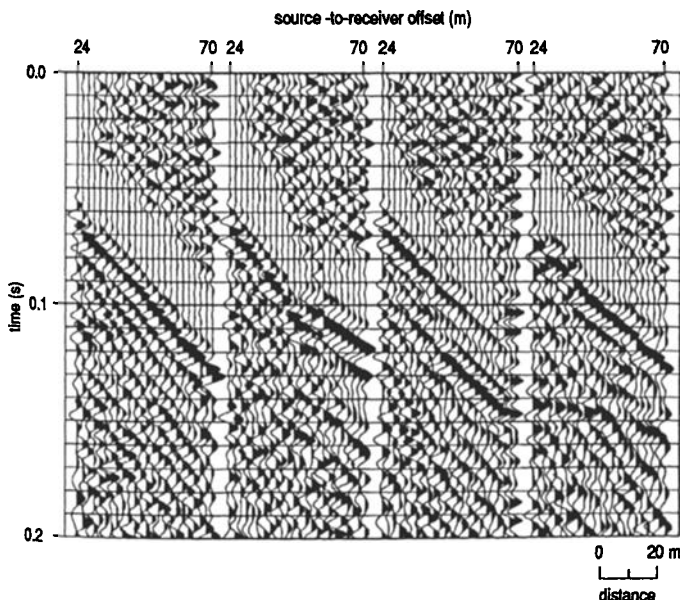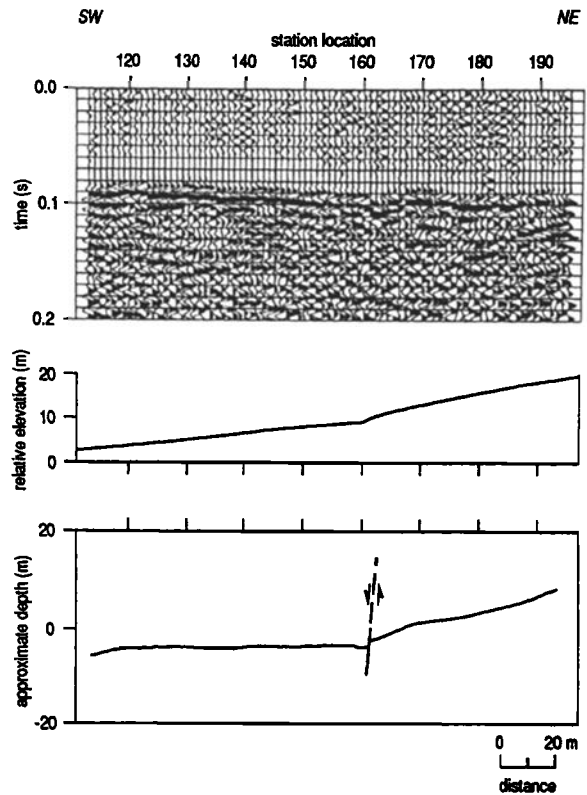

Fig. 5. Disruption in refracted arrivals at locations 161 to 163 on this 46-m common offset section relates with the 1983 earthquake fault scarp.

fault zone at the depth of refractor is interpreted to be 6 m wide. The refraction interpretation (Figure 5) suggests the near-surface interface is 7 to 10 m deep and slopes towards the southwest approximately following the ground surface. In tectonically active areas, disruptions in the continuity of the seismic signal are generally considered to be the result from structural variability. Other possible reasons for the calculated depth variations of this first refracting interface includes lithologic changes in refracting media and changes in the acoustic properties of material between the surface and the interface. Correlating the interpreted fault on the refractor and the scarp suggest normal faulting with a southwest dip.

Results and Discussion

The 130 ms reflection possesses a southwest dip roughly mimicking the surface topography. Reflector depth across the line varies from approximately 74 to 86 m. Reflections disjointed by faulting achieve good correlation and continuity when compensated for offset by physically cutting the CDP stacked section along interpreted faults and sliding along the cuts until reflection wavelets correlate. This observation lends confidence to the interpretation that the reflector has been segmented by faulting and allows a consistent interpretation across the entire line.

Subtle similarities can be observed between interpreted subsurface structure and the surface topography (Figure 3). It is important to note that these similarities are not related to static problems. With the source-receiver offsets used, both the source static and the receiver static are caused by near-surface anomalies that are located at least 12 meters horizontally away from the topographic and subsurface structural anomalies.

Interpreted subsurface faults on Figure 3 with potential subdued expression at the ground surface are probably from previous earthquake activity. Years of erosion and deposition

Fig. 4. Filtered data displaying variability in recorded arrivals.

removed the majority of the surface expression of these seis-
mically identified subsurface geologic features.

Horst-graben-type structures have been interpreted on
seismic data near the Lost River fault at Doublespring Pass
road [Treadway et al., 1988]. Notable changes in reflection
character observed between stations 132-155 and stations 186-
195. These chaotic zones within graben-like structures are
probably the result of tectonically altered material lacking suf-
ficient acoustic contrast and bed competency to generate coher-
ent seismic reflections. Reflection times suggest bedrock at
Arentson Gulch (approximately 80 m) is 2 to 3 times deeper
than along the Lost River fault at Doublespring Pass road.

Previous studies [Crone and Machette, 1984] in conjunc-
tion with our seismic refraction and reflection data suggest the
surface fault is probably related to the group of faults inter-
preted between stations 132 and 160. Total bedrock displace-
ment interpreted along this seismic survey line is approxi-
mately 6 m, representing 4 to 6 times more displacement than
is observed on either the common offset refraction section or at
the surface. This discrepancy is probably indicative of tectonic
activity along the western splay after the top of bedrock was
deposited but before the 7-10 m deep refractor was present.

Comparing the 6 m of displacement on the western splay
with the thousands of meters of displacement that has occurred
along the frontal fault since Oligocene/Miocene time, it
becomes apparent that activity on the western splay is either
extremely rare or was initiated during Quaternary. Another
possibility is that strike-slip motion may locally accommodate
some of the strain resulting in small net dip-slip.

Conclusions

(1) Segmentation of the approximately 80-m deep bedrock
by several faults with total displacement of approximately 6 m
suggests several episodes of tectonic activity in this area,
assuming the 1983 earthquake is characteristic for the area.

(2) Normal faulting seems to have produced graben
structures on the surface of the bedrock.

(3) The fault scarp appears to be related to a fault zone
interpreted on the seismic data between CDPs 265 and 320.

(4) Activity on the western splay is either much younger
or extremely infrequent with respect to the frontal fault (Lost
River fault), or strike-slip motion may be dominant on the
western splay.

(5) Based on small total displacement of bedrock, activity
on the western splay is probably secondary rupturing or
deflection of major activity along the frontal fault used in con-
junction with reflection and surface information.

References

Baldwin, E. W., Faulting in the Lost River Range area of
   Idaho, *American Journal of Science, 249*, 884-902, 1951.
Bilham, R., Subsurface radar imagery of the near-surface
   fractures associated with the Borah Peak earthquake,
   Idaho, Workshop XXVIII on the Borah Peak, Idaho,
   earthquake, vol. A, *U.S. Geological Survey Open-file
   Report 85-290*, 182-194, 1985.
Crone, A. J., and M. N. Machette, Surface faulting accompa-
   nying the Borah Peak earthquake, central Idaho, *Geology,
   12*, 664-667, 1984.
Crone, A. J., M. N. Machette, M. G. Bonilla, J. J.
   Leinkaemper, K. L. Pierce, W. E. Scott, and R. C.
   Bucknam, Characteristics of surface faulting accompany-
   ing Borah Peak Earthquake, central Idaho, Workshop
   XXVIII on the Borah Peak, Idaho, earthquake, vol. A.,
   U.S. Geological Survey Open-file Report 85-290, 43-58,
   1985.
Crone, A. J., M. N. Machette, M. G. Bonilla, J. J.
   Lienkaemper, K. L., Pierce, W. E. Scott, and R. C.
   Bucknam, Surface faulting accompanying the Borah Peak
   earthquake and segmentation of the Lost River fault, cen-
   tral Idaho, *Seismological Society of America Bulletin 77*,
   739-770, 1987.
Hait, M. H., Jr., Doublespring Pass road trench, fault scarps,
   landslides, and other features associated with the Borah
   Peak earthquake of Oct. 28, 1983, central Idaho: A Field-
   trip Guide, *U.S. Geological Survey Open-file Report 85-
   290*, B, 11-17, 1985.
Hait, M. H., Jr., and W. E. Scott, Holocene faulting, Lost
   River Range, Idaho, *Geological Society of America
   Abstract with Programs, 10*, 217, 1978.
Miller, R. D., D. W. Steeples, Shallow structure from a
   seismic-reflection profile across the Borah Peak, Idaho,
   fault scarp, *Geophysical Research Letters, 13*, 953-956,
   1986.
Pullan, S. E., and J. A. Hunter, Seismic model studies of the
   overburden-bedrock reflection, *Geophysics, 50*, 1684-
   1688, 1985.
Scott, W. E., K. L. Pierce, and M. H. Hait, Jr., Quaternary
   tectonic setting of the 1983 Borah Peak earthquake, central
   Idaho, *Seismological Society of America Bulletin 75*,
   1053-1066, 1985.
Treadway, J. A., D. W. Steeples, and R. D. Miller, Shallow
   seismic study of a fault scarp near Borah Peak, Idaho,
   Journal of Geophysical Research, 93(B6), 6325-6337,
   1988.

Mubarik Ali, Quaid-i-Azam University, Islamabad,
Pakistan
   Richard D. Miller and Don W. Steeples, Kansas
Geological Survey, University of Kansas, Lawrence, KS
66047